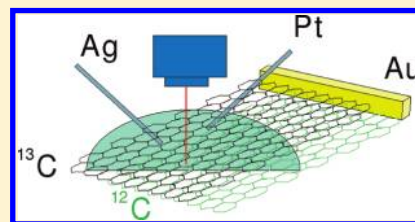


Raman Spectroscopy and in Situ Raman Spectroelectrochemistry of Bilayer $^{12}\text{C}/^{13}\text{C}$ GrapheneMartin Kalbac,^{*,†,§} Hootan Farhat,[‡] Jing Kong,[§] Pavel Janda,[†] Ladislav Kavan,[†] and Mildred S. Dresselhaus^{§,||}[†]J. Heyrovský Institute of Physical Chemistry, Academy of Sciences of the Czech Republic, v.v.i., Dolejškova 3, CZ-18223 Prague 8, Czech Republic[‡]Department of Materials Science and Engineering, [§]Department of Electrical Engineering and Computer Science, and^{||}Department of Physics, Massachusetts Institute of Technology, Cambridge, Massachusetts 02139, United States

S Supporting Information

ABSTRACT: Bilayer graphene was prepared by the subsequent deposition of a ^{13}C single-layer graphene and a ^{12}C single-layer graphene on top of a SiO_2/Si substrate. The bilayer graphene thus prepared was studied using Raman spectroscopy and in situ Raman spectroelectrochemistry. The Raman frequencies of the ^{13}C graphene bands are significantly shifted with respect to those of ^{12}C graphene, which allows us to investigate the single layer components of bilayer graphene individually. It is shown that the bottom layer of the bilayer graphene is significantly doped from the substrate, while the top layer does not exhibit a signature of the doping from the environment. The electrochemical doping has the same effect on the charge carrier concentration at the top and the bottom layer despite the top layer being the only layer in contact with the electrolyte. This is here demonstrated by essentially the same frequency shifts of the G and G' bands as a function of the electrode potential for both the top and bottom layers. Nevertheless, analysis of the intensity of the Raman modes showed an anomalous bleaching of the Raman intensity of the G mode with increasing electrode potential, which was not observed previously in one-layer graphene.



KEYWORDS: Graphene, bilayer, Raman spectroscopy, spectroelectrochemistry, electrochemical charging

Graphene is a two-dimensional (2D) material which has attracted attention due to its unique properties that are promising for applications in nanoelectronics. One of the great advantages of graphene is a tunability of its transport and optical properties by doping. This provides an important degree of freedom which broadens the area of prospective applications of this simple and fundamental new material.

Doping of graphene can be achieved by the interaction with chemicals,¹ by electrochemistry,^{2,3} or by electrostatic backgating^{4–6} through a substrate. Electrochemical or electrostatic doping provides an easy way to control the Fermi level of graphene which makes these methods attractive for applications. Electrostatic back gating is simple and there is a clear application link toward FETs (field-effect transistors). However, the electrostatic doping depends on the properties of the dielectric. The doping efficiency is typically very low, and for this reason a high voltage (up to 100 V) must be used. In addition the doping is complicated by the presence of trapped charges in the dielectric serving as a substrate.⁷ Electrochemical doping, on the other hand, is more efficient, so that a voltage of ± 1.5 V is usually sufficient to get a significant doping level. The charge is here mediated by an Ohmic contact to the sample and it is compensated by electrolyte counterions, which avoid problems with trapped charges. Nevertheless, the experiments are usually more difficult to carry out since the electrochemical setup brings specific requirements for the cell geometry, the quality of the electrodes, and the purity of the chemicals. Also to achieve good

control of the applied voltage, a three-electrode potentiostatic system must be used.⁸

Raman spectroscopy provides a convenient tool for characterizing graphene, since it can distinguish between single-layer (1-LG), bilayer (2-LG), and multilayer graphene, and Raman spectroscopy is also highly sensitive to the electronic structure of these materials.⁹ The important features observed in the Raman spectra are the G mode and the G' mode (also sometimes called the 2D mode¹⁰). The G and G' modes are present in all graphene-based materials; however, their frequencies, intensities, and line widths are influenced by other factors like the number of graphene layers, the external/intentional doping or unintentional doping, stress, and the laser excitation energy. In some graphene samples, the D line is also found and the D line is believed to indicate the presence of defects¹¹ as in ordinary graphite.

Recent advances in chemical vapor deposition (CVD) synthesis now allow the preparation of large and uniform single-layer graphene flakes.^{12,13} Previous Raman studies made on CVD grown graphene¹⁴ showed that electrochemical doping leads to a change of the width, frequency, and intensity of the Raman signal.² Very interesting are also the observed changes in the intensity of the graphene Raman bands during doping.^{2,3,14,15} For example, recent experimental results and theoretical calculations pointed to an anomalous enhancement of the Raman G

Received: January 18, 2011

Revised: April 2, 2011

Published: April 20, 2011

band at highly positive potentials.^{14,16} This effect could be important, for example, in the identification of single-layer graphene samples in a charged state.

In bilayer graphene with AB stacked layers a tunable band gap can be opened by an electric field^{17–20} which makes this material very attractive for applications in nanoelectronics. The different electronic structure of bilayer graphene is also reflected in its different characteristic Raman spectra and their dependence on electrical charging as compared to single-layer graphene.¹⁵ For applications in nanoelectronics it is also interesting to analyze the charge distribution between graphene layers.¹⁵ However, in the bilayer graphene with AB stacked layers the studies of charge transfer between layers are complicated by a coupling between the layers. In addition the analysis of the Raman spectra of bilayer graphene during the doping is difficult due to the fact that the Raman features belonging to the top and bottom layers overlap. Hence it is very challenging to follow the response to the electrode potential of the top and the bottom layers individually in bilayer graphene.

In the present paper we examine, for the first time, the Raman spectra of the two layers of bilayer graphene in which one layer is of natural isotope composition (mostly of ¹²C atoms) and the second layer is labeled by the ¹³C isotope. We investigated this material both in its neutral and in doped states. This isotopic labeling allowed us to follow the Raman spectra of the two components (the top and bottom layer) of bilayer graphene separately.

Panel a of Figure 1 shows an optical microscope image of single layer graphene and two-layered graphene on a SiO₂/Si substrate in a single photograph. There is a clear change of the optical absorption between 1-LG and 2-LG which simplifies the identification of a particular part of the sample with 1-LG and another part with 2-LG. Panel b of Figure 1 shows an atomic force microscopy (AFM) picture of the bottom layer and the top layer. The step between the substrate and the 1-LG and the step between the first layer and the second layer are in the range between 0.5 and 1 nm, which is similar to that measured for 1-LG and 2-LG prepared by the exfoliation method²¹ and our measurement of 2-LG synthesized by CVD method. However, the accuracy of the evaluation of the step size was limited by the underlying surface oxide, since the graphene copies the SiO₂ grains to some extent. Also the edges of graphene tend to fold. This effect is especially frequent in the case of the second graphene layer where it is almost impossible to find unfolded edges. The top layer contains significantly more wrinkles. This might be because there are “intrinsic wrinkles” of the top layer, and in addition the top layer copies the wrinkles of the bottom layer. Another reason could be the weaker interaction between top graphene layer and the bottom graphene layer compared to that of bottom layer and SiO₂. In the former case the weaker interaction will allow the formation of a wrinkle to release the local stress of the graphene layer.

We note that on a macroscopic scale the edge parts of the whole graphene layer may contain some “transfer” residuals which are difficult to remove. Nevertheless the sample size is large, and therefore it is easy to avoid the edge parts of the graphene sample. Furthermore the PMMA residuals would be composed from the ¹²C isotope, and hence they will interfere with the Raman spectra of the ¹²C layer. As we show later in this study both top and bottom layers exhibit similar behaviors; therefore it is very unlikely that PMMA residuals contribute to our Raman spectra.

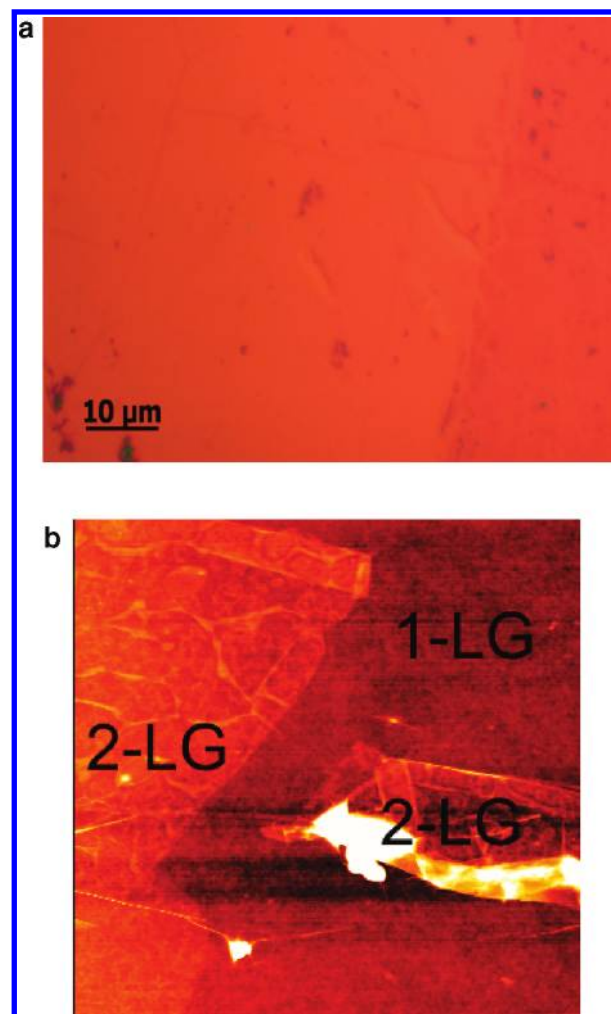


Figure 1. (a) An optical microscope image of 1-LG over most of the image and 2-LG is seen on the right part of the image. (b) AFM topography of the 1-LG and 2-LG. Scan size is 2.0 μm × 2.0 μm.

Figure 2 shows the Raman spectra of 2-LG in comparison to that of ¹²C 1-LG (note that the ¹²C sample is expected to contain the natural isotopic abundance, that is 1.07% of ¹³C) and to that of ¹³C 1-LG (in which the ¹³C content is 99% taken from the declared precursor's purity). The Raman spectrum of the ¹³C 1-LG sample exhibits the same Raman features as the Raman spectrum of the ¹²C 1-LG except for a downshift of all the Raman bands for the ¹³C 1-LG sample. The observed downshifts of the D, the G and the G' bands for the ¹³C graphene with respect to those of the ¹²C graphene are about 52, 60, and 100 cm^{−1}, respectively. In a continuum model, the frequency shift of the Raman bands in the ¹³C enriched material originates from the increased mass of this isotope which is given by eq 1:

$$(\omega_0 - \omega)/\omega_0 = 1 - [(12 + c_0)/(12 + c)]^{1/2} \quad (1)$$

where ω_0 is the frequency of a particular Raman mode in the ¹²C sample, $c = 0.99$ is the concentration of ¹³C in the enriched sample, and $c_0 = 0.0107$ is the natural abundance of ¹³C. According to eq 1, the downshift of the D, the G, and the G' bands is expected to be 48, 56, and 95 cm^{−1}, respectively, which is in quite good agreement with our experimental results.

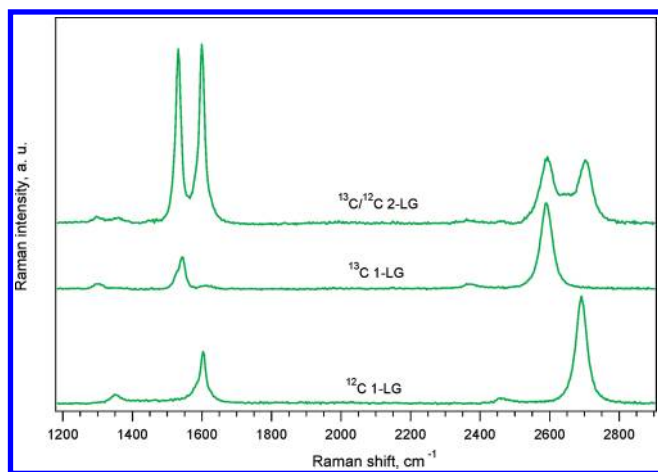


Figure 2. Raman spectra of the ^{12}C 1-LG, ^{13}C 1-LG, and $^{13}\text{C}/^{12}\text{C}$ 2-LG (^{13}C is on top, ^{12}C at bottom) samples. The spectra are excited using 2.33 eV laser excitation energy.

The 2-LG sample is composed of the ^{12}C 1-LG on the bottom layer and the ^{13}C 1-LG on the top layer relative to the SiO_2 substrate. Two components of the G band and the G' band, corresponding to the top and the bottom layers, are clearly distinguished in Figure 2. One can also trace two D bands, each corresponding to the top and the bottom layers. It is clear that the spectrum of 2-LG is not a simple superposition of the ^{12}C 1-LG and the ^{13}C 1-LG spectra. The top layer of the 2-LG sample composed of ^{13}C atoms exhibits a downshift of the G mode (by about 10 cm^{-1}) as compared to the G mode in the ^{13}C 1-LG spectrum. The downshift cannot be attributed to an isotope exchange between ^{12}C 1-LG and the ^{13}C 1-LG during the fabrication process of the 2-LG since in such a case an upshift of the Raman bands would be observed. Hence, we conclude that the SiO_2 substrate causes a local doping of the graphene which leads to an upshift of the Raman bands of the ^{13}C top layer in 2-LG as compared to the ^{13}C layer in 1-LG. The ^{13}C top layer of the 2-LG sample is not contacting SiO_2 , and therefore the doping effect is absent and the Raman spectra are different from those measured on the ^{13}C 1-LG sample deposited directly on SiO_2 , which has puddles of electrons and holes.²² Results are also consistent with those reported previously on 1-LG.²³ In addition it has been shown recently that the heat treatment of graphene on a SiO_2 substrate causes changes in the Raman spectra due to more intimate contact.²⁴ The transfer process in our case also required a heating procedure to remove residuals of PMMA. In general, it is difficult to distinguish the specific role of the temperature-induced interaction of graphene with SiO_2 from the effects of thermal treatment of graphene by studying samples of 1-LG or 2-LG with the natural abundance of ^{12}C . In our study the combination of ^{13}C and ^{12}C layers provides an excellent tool to monitor the substrate interactions, since the bottom and top layers can be clearly distinguished. Obviously the bottom layer exhibits more significant doping than the top layer, and therefore we can confirm that “the heating effects” come from the interaction of SiO_2 with graphene.

The frequency of the G mode is identical for the ^{12}C bottom layer in the 2-LG sample and in the ^{12}C 1-LG sample. Both the ^{12}C bottom layer and the ^{12}C 1-LG are in contact with the SiO_2 substrate. However, the ^{12}C bottom layer in the 2-LG sample is protected from the environment, which may also cause a doping

of graphene. Since there is no significant difference in the G mode position, we suggest that for our experimental setup the extent of the doping via adsorbed molecules coming from the environment (like oxygen and water from the air) is negligible compared to the doping from the substrate.

The G' band frequency of the ^{13}C top layer in the 2-LG sample is found at about 2594 cm^{-1} which is similar to that for the G' band in the ^{13}C 1-LG (2591 cm^{-1}) sample. For the ^{12}C bottom layer of the 2-LG sample, we found the G' mode frequency at 2704 cm^{-1} ; hence it is considerably upshifted relative to the value of 2691 cm^{-1} found for the ^{12}C 1-LG sample. Taking into account the isotopic shift of the G' mode and a change of the position of the G' mode for the ^{12}C layer, the G' mode frequency of the ^{13}C top layer should be at about 2694 cm^{-1} . Hence, the experimental value of the G' mode is at least 10 cm^{-1} higher than that expected for a noninteracting layer. In contrast to the G mode, the G' mode frequency is only weakly dependent on the doping (vide infra). Therefore the observed shift cannot be fully explained by a different charge state of the 1-LG and the top layer of the 2-LG sample. Hence, we attribute the observed G' band shift to the local change in the stress of the graphene sheet. We assume that the top layer of graphene is more relaxed due to weak van der Waals interactions which allow a sliding of graphene layers. On the other hand, strong interactions between the SiO_2 substrate and graphene layers create stress in the graphene. In addition, the SiO_2 has an opposite sign of its thermal expansion coefficient relative to that of graphene so that each heating process creates mechanical stress in the graphene layer attached to the SiO_2 substrate. The stress causes a downshift of the Raman G' mode, and an upshift is observed for the more relaxed top layer of the 2-LG sample which is in agreement with previous results. The magnitude of the shift (10 cm^{-1}) corresponds to a stress of about 0.2%.²⁵

Finally, there is also a large change in the intensities of the Raman bands when comparing the Raman signal of the 2-LG and the 1-LG samples: (1) The absolute intensity of the G band is increased in the 2-LG graphene sample with respect to the G band in the 1-LG sample, and (2) the peak height ratio G/G' is increased for the 2-LG graphene sample relative to that for the 1-LG sample. The Raman bands of the G' mode are broadened for the 2-LG sample which may partly explain a change in the G/G' ratio. Nevertheless, even if the peak areas are compared, the G/G' ratio is increased for the 2-LG graphene sample relative to that for the 1-LG sample. A different G/G' ratio is also a typical feature distinguishing 1-LG from 2-LG. The change in the absolute intensity of the Raman spectra may be attributed to an interference effect,²⁶ to a surface enhancement effect in graphene known as graphene-enhanced Raman spectroscopy (GERS),^{27–30} or to a specific electronic structure of slightly rotated graphene layers.^{31,32} The interference effects would lead to an enhancement of all Raman modes while the GERS effect can be selective. Obviously the enhancement of the G mode is stronger than that of the G' mode which supports GERS as an enhancement mechanism. The intensity of the G mode in the 2-LG sample is increased similarly for both the top and the bottom layer compared to that for the 1-LG sample (Figure 2). It was shown recently that the Raman signal of molecules attached to graphene can be strongly enhanced due to the chemical mechanism of GERS.^{27,28} The distance between the layers is assumed to be about 0.335 nm, which is small enough to observe the enhancement effect. Nevertheless, the enhancement of the Raman spectra of the graphene layer by another graphene layer

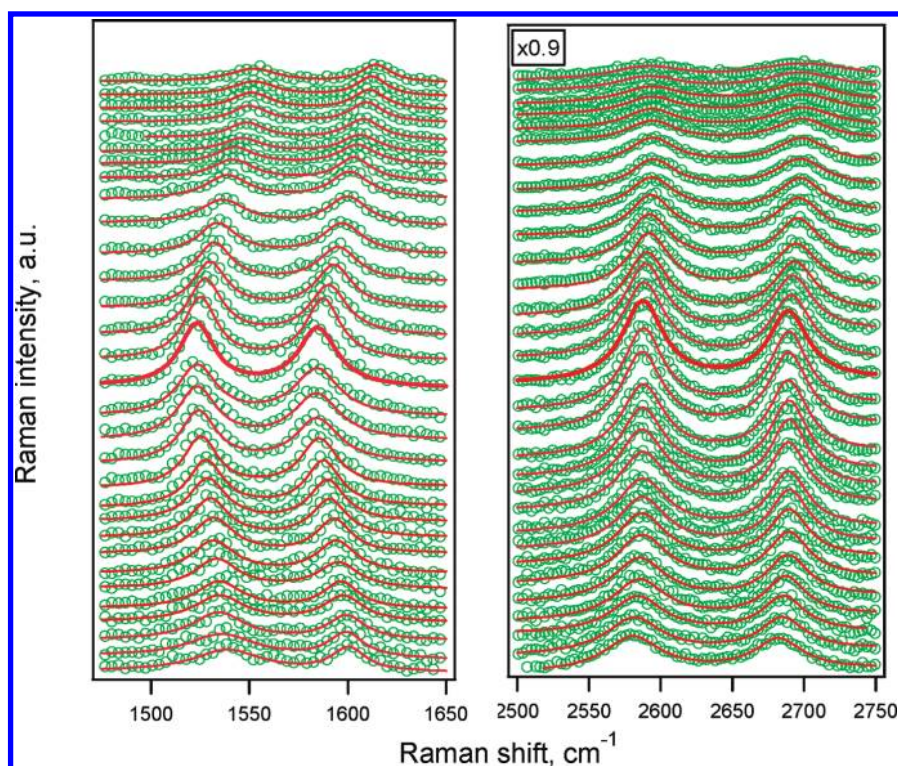


Figure 3. In situ Raman spectroelectrochemistry of the G-band (left) and the G' -band of a 2-LG sample. The spectra are excited by 2.33 eV laser excitation energy and the electrode potentials range from -1.5 to 1.5 V vs Ag/Ag^+ (from bottom to top) with a step of 0.1 V. The empty circles represent the experimental points and the solid lines their fit with a Lorentzian line shape.

has not been discussed in the literature yet. The reason can be the absence of the enhancement in 2-LG with AB stacked layers. The electronic coupling between the layers of the latter material results in a new electronic structure of 2-LG with AB stacked layers. The chemical enhancement is however sensitive to changes in electronic structure, and hence the coupling of layers may bring the AB stacked 2-LG out of the resonance condition.³³

Finally, it has been shown recently that even samples without perfect AB stacking of the graphene layers exhibit some modification of their electronic structure.^{31,32} In particular, a small rotation of the graphene layers leads to a flattening of the electronic bands which may lead to the enhancement of the Raman signal due to an increased density of states.^{31,32}

In order to follow the behavior of the 2-LG Raman spectra in a charged state, we performed in situ Raman spectroelectrochemical measurements. In these experiments the potential was changed from 0 to -1.5 to 1.5 V with steps of 0.1 V between the traces in Figure 3. Here the positive and negative signs of the electrode potentials correspond to hole and electron doping, respectively. At each potential step the Raman spectrum was measured, while keeping the potential constant. We also emphasize that in our experiments, we use a three electrode system with a potentiostat, which ensures good control of the applied potential.

Figure 3 shows in situ Raman spectroelectrochemical data measured on the 2-LG samples in which the bottom layer (contacting SiO_2) was graphene with a natural isotope composition and the top-layer was labeled by ^{13}C (as in Figure 2). The spectra are excited using 2.33 eV laser excitation energy. At an electrode potential of 0 V, the bands at about 1522 , 1583 , 2588 , and 2688 cm^{-1} correspond to the G band of the ^{13}C layer, the G band of the ^{12}C layer, the G' band of the ^{13}C layer, and the G'

band of the ^{12}C layer, respectively. The electrochemical doping causes significant changes of the Raman intensities and frequencies of the G and the G' modes both for the ^{12}C layer and for the ^{13}C layer.

The G band of the ^{12}C layer is shifted from 1583 at 0 V to 1615 cm^{-1} at $+1.5$ V (32 cm^{-1}) and to 1600 cm^{-1} at -1.5 V (17 cm^{-1}). For the ^{13}C top layer the G band is shifted from 1522 to 1555 cm^{-1} (33 cm^{-1}) and to 1539 cm^{-1} for -1.5 V (17 cm^{-1}). Hence there is no significant difference between the dependence of the G band frequency on electrode potential for the top and the bottom layers, respectively. The observed values of the frequency shift of the G mode in 2-LG upon electrochemical doping are consistent with the data obtained for 1-LG graphene.^{2,15} The observed dependence of the frequency shift of the G mode is slightly different for positive and negative signs of charging. This allows us to distinguish from the spectra whether the graphene layer is charged positively or negatively. In our configuration the development of the G mode is similar for both the top and the bottom layers, which confirms the same sign of doping for both layers.

The G' mode frequency is also expected to change if the sample is doped. In the case of the ^{12}C layer sample, the measurements show that the G' band frequency is shifted from 2688 cm^{-1} at 0 V to 2697 cm^{-1} at $+1.5$ V (9 cm^{-1}) and to 2683 cm^{-1} at -1.5 V (-5 cm^{-1}), while for the ^{13}C layer sample, the G' mode frequency is changed from 2588 cm^{-1} at 0 V to 2597 cm^{-1} at 1.5 V (9 cm^{-1}) and to 2582 cm^{-1} at -1.5 V (-6 cm^{-1}). Hence, it can be concluded that the development of the G' mode is similar for both the top and the bottom layers of the 2-LG sample.

The same electrode potential dependence of the frequency of the G and the G' modes for the ^{13}C and the ^{12}C layers in the 2-LG

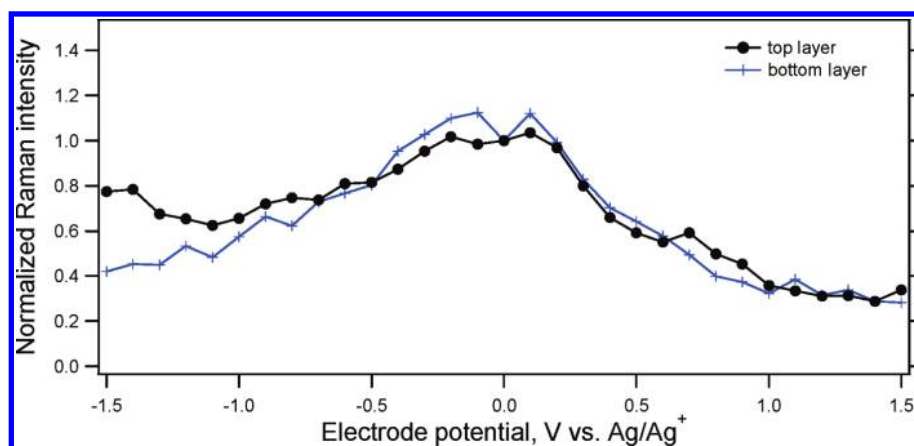


Figure 4. The G mode area (from a Lorentzian fit of the Raman spectra) dependence on electrode potential. The circles correspond to the ^{13}C top layer while the crosses correspond to the ^{12}C bottom layer in the 2-LG sample. The area at each potential is normalized to the area at 0 V. The Raman spectra are excited by 2.33 eV laser excitation energy.

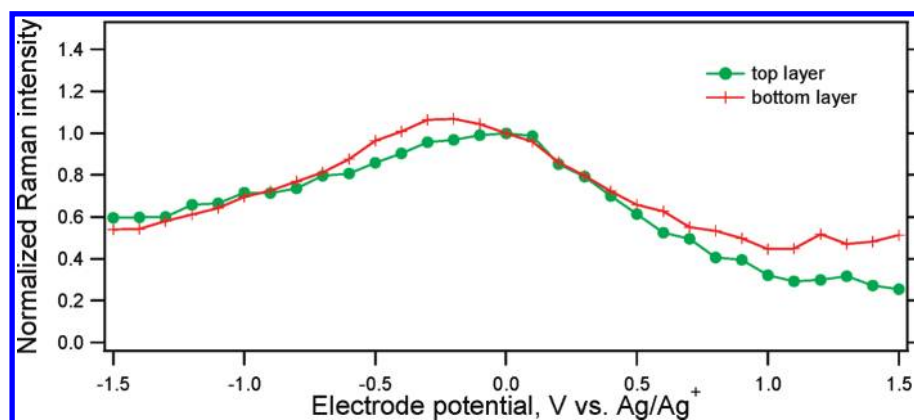


Figure 5. The G' mode area in 2-LG (from a Lorentzian fit of the Raman spectra) dependence on electrode potential. The circles correspond to the ^{13}C top layer while the crosses to the ^{12}C bottom layer in the 2-LG sample. The area at each potential is normalized to the area at 0 V. The Raman spectra are excited by 2.33 eV laser excitation energy.

sample indicates the same amount of charge on both layers at each probed potential. It is important to note that only the top layer is in contact with the electrolyte while both the top and bottom layers are in Ohmic contact. The electronic charge of the bottom layer must be therefore compensated by the electrolyte counterions through the top layer only. The same behavior of the top and bottom graphene layers in 2-LG means that the effect of the electrolyte is weak. (The top layer reflects both the effect of the electric field and the double layer formed at the interface between the graphene and the electrolyte, while the bottom layer reflects only the changes induced by the electric field.) Intercalation of Li^+ between the layers is, obviously, excluded, even at -1.5 V.

These results also support our assumption that the shift of the G' mode in the ^{13}C layer of the 2-LG sample is caused by stress, because the frequency of the G' mode for both the ^{13}C and the ^{12}C layers shows the same dependence on electrode potential.

The situation in 2-LG is to some extent reminiscent of the doping response of double-walled carbon nanotubes (DWCNT) which, however, showed much more pronounced differences in the doping behavior of the inner and outer tubes.³⁴ Possible different variations of the electronic type (metallic, semiconducting) of the inner and outer tubes make the interpretation of the

behavior of the DWCNTs during doping relatively complex.³⁴ Nevertheless the comparison of 2-LG and DWCNTs points to an important effect of the Ohmic contact on both layers, which is missing in DWCNTs.³⁴

It is obvious from Figure 3 that the intensities of the Raman bands change by doping. Nevertheless, previous studies on 1-LG samples showed that the width of the Raman bands is also changing as a function of doping.¹⁴ Therefore to determine the intensity changes of the Raman bands more accurately, one should evaluate the area of the Raman bands rather than peak heights. The measured dependences of the peak areas on electrode potentials for the G and the G' modes in the 2-LG samples are shown in Figures 4 and 5, respectively. Obviously the peak areas of the G band and of the G' band are decreasing as the doping is increased for both positive and negative potentials. Let us focus on the G band first. Figure 4 compares the Raman intensities (areas) of the G mode for the ^{13}C layer (top) and the ^{12}C layer (bottom) of the 2-LG sample with regard to its dependence on electrode potential. Obviously, the G band areas in both the top and the bottom layers in the 2-LG sample decrease similarly. The orientation of the two graphene layers is presumably random, and therefore no coupling between the two layers due to AB stacking order should be expected. Consequently, the

2-LG sample should behave in the same way as the 1-LG sample as far as the doping is concerned. For 1-LG a significant drop of the G-band peak height at around 0 V is often observed.^{14,35,36} However, in this case the change in peak height is obviously related to the broadening of the G band.³⁵ In undoped samples the phonons can dissipate energy by forming an electron–hole pair.^{35,36} In doped samples this process is suppressed because the final state is occupied (for electron doping) or it is empty (for p doping) and therefore the G band is narrowed.^{6,35,36} By further doping, the peak height is not changed up to about 1.0 V where some anomalous effects can be observed.¹⁴ Here in this study we used the area under the G feature for the evaluation of the G mode intensity dependence on electrode potential. In the 1-LG sample the change of the peak height is compensated by a change in the peak full width at half maximum; hence the peak area is essentially constant as a function of the potential from 0 to ± 1 V.¹⁴ However, the behavior of the 2-LG sample is in strong contrast to the behavior of the G mode in 1-LG graphene.¹⁴ Note, that we tested also a part of the same sample which was covered only by 1-LG (cf. Figure 1). In this case no significant change in the area was observed except for very high positive potentials where an increase of the intensity was found (data not shown). The reason for the anomalous intensity decrease of the G mode in the case of 2-LG could be a change in the electronic coupling of the layers due to Coulomb repulsion of the layers. (The electrochemical doping leads to the charging of layers with the same sign of charge carriers.) As discussed above, the interaction between layers with a small angle of rotation may cause the appearance of Van Hove singularities in the electronic structure of graphene and/or flattening of the electronic bands.^{31,37} A doping-induced decoupling of the layers may return the electronic structure to the linear dispersion as found in the 1-LG and thus canceling any enhancement effects caused by the interaction between two graphene layers.

The decrease of intensity may perhaps be also attributed to a smaller GERS^{27–30} enhancement for a doped sample compared to a pristine sample. A shift of the Fermi level prevents the formation of e–h pairs and it also leads to a change in the electronic structure of graphene.³⁸ This may bring the doped graphene bilayer out of resonance.³³ The GERS effect is not expected for 1-LG itself; hence no bleaching of the Raman bands should be observed in this case, which is consistent with previous results.¹⁴

Figure 5 shows the measured dependence of the area of the G' mode on the electrode potential for both the ¹³C and the ¹²C layers in the 2-LG sample. The area $A_{G'}$ of the ¹³C layer reaches its maximum at a potential of about 0 V while for the bottom layer, the maximum intensity is slightly shifted by -0.2 V, which is consistent with the proposed slight doping of the bottom graphene layer from the substrate. The slope of the intensity decrease is similar to that observed previously for the 1-LG sample.¹⁴ It has been suggested already that the area of the G' band ($A_{G'}$) for the 1-LG sample is proportional to the electron/hole inelastic scattering rate.³ Doping will increase the number of charge carriers and therefore the probability of a scattering event will also increase and the G' band intensity should therefore decrease.³

The dependence of $A_{G'}$ on the electrode potential is somewhat asymmetric for both the bottom and the top layer in the 2-LG sample. This effect therefore cannot be attributed to the substrate since only the bottom layer is in contact with the substrate. The asymmetric dependence was already observed previously for the 1-LG sample.¹⁴ The asymmetry in both the G band and the G' band intensity versus electrode potential curves can be attributed to the relaxation time of the photoexcited

carriers. In the case of negative doping, electrons occupy the π^* band. Thus the relaxation of the photoexcited carriers becomes slow. In the case of hole doping, the states below the Dirac point are empty and the relaxation is fast. This explanation would predict a larger asymmetry for a lower laser excitation energies since the photoexcited carriers are then generated closer to the Dirac point. The effect seems to be more evident for the ¹³C top layer which can be caused by an absence of interaction with the SiO₂ substrate. (The interaction with the substrate may lead to an additional asymmetry of the doping behavior which may compensate for the asymmetry caused by the relaxation of the photoexcited carriers.)

In conclusion we studied a 2-LG sample which was prepared by a subsequent transfer of the ¹²C 1-LG and the ¹³C 1-LG on a SiO₂ substrate. The isotopic shift of the Raman bands of the ¹³C layer compared to that for the ¹²C layer allowed us to study the difference in the doping effects of the individual layers. We found that the bottom layer is doped by the substrate and is also stressed compared to the top layer. The anomalous increase of the G mode intensity in 2-LG compared to 1-LG is tentatively attributed to the weak electronic coupling between graphene layers. In addition, we measured the Raman spectra of 2-LG at different electrode potentials. Our study revealed several interesting phenomena: The electrochemical doping has the same effect on the top layer and on the bottom layer even though only the top layer is in contact with the electrolyte. This was demonstrated by essentially the same shift of the G and G' band frequencies with electrode potential for both the top and bottom layers. An analysis of the change of the intensities of the Raman modes showed an anomalous bleaching of the Raman intensity of the G mode with increasing magnitudes of the electrode potential, which has not been observed for 1-LG. This may point to a reduced interaction of graphene layers by doping. Nevertheless, more experimental and theoretical studies are needed to fully explain these anomalous phenomena. It is important to stress that the layers in our sample are presumably not AB stacked. For AB stacked samples there is a relatively stronger electronic coupling between graphene layers causing a large modification of the electronic structure. It has been shown recently that even samples that do not have perfect AB stacking of the graphene layers exhibit a modification of their electronic structure.^{31,32} In particular for rotation angles between 1 and 2°, new low-energy Van Hove singularities and a flattening of the electronic bands were observed.^{31,37} For larger rotation angles the electronic coupling vanishes; nevertheless the electronic structure is slightly modified up to rotation angles of about 10°. ³⁷ The CVD samples are composed of grains with typical sizes of several μm^2 , which generally have different orientations.¹² The combination of two such layers leads to many different relative orientations of individual grains within a macroscopic 2-LG sample. Since the relative orientations are random, it may be expected that the overall electronic coupling between the layers can be weak but still present. The comparison of our results to AB stacked 2-LG will be very interesting since it will clearly show the role of the coupling for charge transfer. Unfortunately the current state of the art in the field does not allow us to make AB stacked graphene with different isotopes.

■ ASSOCIATED CONTENT

S Supporting Information. Experimental details and the identification of 2-LG. This material is available free of charge via the Internet at <http://pubs.acs.org>.

AUTHOR INFORMATION

Corresponding Author

*E-mail: kalbac@jh-inst.cas.cz.

ACKNOWLEDGMENT

This work (by M.K.) was supported by the Academy of Sciences of the Czech Republic (Contract No. IAA400400911, IAA400400804, and KAN200100801), Czech Ministry of Education, Youth and sports (ME09060 and LC-510), and Czech Grant Agency (203/07/J067, P204/10/1677). The work done at MIT has been supported by NSF-DMR 10-04147.

REFERENCES

- Jung, N.; Kim, N.; Jockusch, S.; Turro, N. J.; Kim, P.; Brus, L. Charge Transfer Chemical Doping of Few Layer Graphenes: Charge Distribution and Band Gap Formation. *Nano Lett.* **2009**, *9* (12), 4133–4137.
- Das, A.; Pisana, S.; Chakraborty, B.; Piscanec, S.; Saha, S. K.; Waghmare, U. V.; Novoselov, K. S.; Krishnamurthy, H. R.; Geim, A. K.; Ferrari, A. C.; Sood, A. K. Monitoring dopants by Raman scattering in an electrochemically top-gated graphene transistor. *Nat. Nanotechnol.* **2008**, *3* (4), 210–215.
- Basko, D. M.; Piscanec, S.; Ferrari, A. C. Electron-electron interactions and doping dependence of the two-phonon Raman intensity in graphene. *Phys. Rev. B* **2009**, *80* (16), 165413.
- Freitag, M.; Steiner, M.; Martin, Y.; Perebeinos, V.; Chen, Z. H.; Tsang, J. C.; Avouris, P. Energy Dissipation in Graphene Field-Effect Transistors. *Nano Lett.* **2009**, *9* (5), 1883–1888.
- Malard, L. M.; Pimenta, M. A.; Dresselhaus, G.; Dresselhaus, M. S. Raman spectroscopy in graphene. *Phys. Rep.* **2009**, *473* (5–6), 51–87.
- Yan, J.; Zhang, Y. B.; Kim, P.; Pinczuk, A. Electric field effect tuning of electron-phonon coupling in graphene. *Phys. Rev. Lett.* **2007**, *98* (16), 166802.
- Zhu, J.; Jhaveri, R.; Woo, J. C. S. The effect of traps on the performance of graphene field-effect transistors. *Appl. Phys. Lett.* **2010**, *96* (19), 193503.
- Kavan, L.; Kalbac, M.; Zukalova, M.; Dunsch, L. Comment on "Determination of the exciton binding energy in single-walled carbon nanotubes. *Phys. Rev. Lett.* **2007**, *98* (1), 019701.
- Ferrari, A. C.; Meyer, J. C.; Scardaci, V.; Casiraghi, C.; Lazzeri, M.; Mauri, F.; Piscanec, S.; Jiang, D.; Novoselov, K. S.; Roth, S.; Geim, A. K. Raman spectrum of graphene and graphene layers. *Phys. Rev. Lett.* **2006**, *97* (18), 187401.
- Thomsen, C.; Reich, S. Double resonant Raman scattering in graphite. *Phys. Rev. Lett.* **2000**, *85* (24), 5214–5217.
- Lucchesi, M. M.; Stavale, F.; Ferreira, E. H. M.; Vilani, C.; Moutinho, M. V. O.; Capaz, R. B.; Achete, C. A.; Jorio, A. Quantifying ion-induced defects and Raman relaxation length in graphene. *Carbon* **2010**, *48* (5), 1592–1597.
- Li, X. S.; Cai, W. W.; An, J. H.; Kim, S.; Nah, J.; Yang, D. X.; Piner, R.; Velamakanni, A.; Jung, I.; Tutuc, E.; Banerjee, S. K.; Colombo, L.; Ruoff, R. S. Large-Area Synthesis of High-Quality and Uniform Graphene Films on Copper Foils. *Science* **2009**, *324* (5932), 1312–1314.
- Reina, A.; Jia, X. T.; Ho, J.; Nezhich, D.; Son, H. B.; Bulovic, V.; Dresselhaus, M. S.; Kong, J. Large Area, Few-Layer Graphene Films on Arbitrary Substrates by Chemical Vapor Deposition. *Nano Lett.* **2009**, *9* (1), 30–35.
- Kalbac, M.; Reina-Cecco, A.; Farhat, H.; Kong, J.; Kavan, L.; Dresselhaus, M. S. The Influence of Strong Electron and Hole Doping on the Raman Intensity of Chemical Vapor-Deposition Graphene. *ACS Nano* **2010**, *4* (10), 6055–6063.
- Das, A.; Chakraborty, B.; Piscanec, S.; Pisana, S.; Sood, A. K.; Ferrari, A. C. Phonon renormalization in doped bilayer graphene. *Phys. Rev. B* **2009**, *79* (15), 155417.
- Basko, D. M. Calculation of the Raman G peak intensity in monolayer graphene: role of Ward identities. *New J. Phys.* **2009**, *11*, 095011.
- McCann, E. Asymmetry gap in the electronic band structure of bilayer graphene. *Phys. Rev. B* **2006**, *74* (16), 161403.
- Castro, E. V.; Novoselov, K. S.; Morozov, S. V.; Peres, N. M. R.; Dos Santos, J. M. B. L.; Nilsson, J.; Guinea, F.; Geim, A. K.; Neto, A. H. C. Biased bilayer graphene: Semiconductor with a gap tunable by the electric field effect. *Phys. Rev. Lett.* **2007**, *99* (21), 216802.
- Zhang, Y. B.; Tang, T. T.; Girit, C.; Hao, Z.; Martin, M. C.; Zettl, A.; Crommie, M. F.; Shen, Y. R.; Wang, F. Direct observation of a widely tunable bandgap in bilayer graphene. *Nature* **2009**, *459* (7248), 820–823.
- Oostinga, J. B.; Heersche, H. B.; Liu, X. L.; Morpurgo, A. F.; Vandersypen, L. M. K. Gate-induced insulating state in bilayer graphene devices. *Nat. Mater.* **2008**, *7* (2), 151–157.
- Ishigami, M.; Chen, J. H.; Cullen, W. G.; Fuhrer, M. S.; Williams, E. D. Atomic structure of graphene on SiO₂. *Nano Lett.* **2007**, *7* (6), 1643–1648.
- Zhang, Y. B.; Brar, V. W.; Girit, C.; Zettl, A.; Crommie, M. F. Origin of spatial charge inhomogeneity in graphene. *Nat. Phys.* **2009**, *5* (10), 722–726.
- Shi, Y. M.; Dong, X. C.; Chen, P.; Wang, J. L.; Li, L. J. Effective doping of single-layer graphene from underlying SiO₂ substrates. *Phys. Rev. B* **2009**, *79* (11), 115402.
- Cheng, Z.; Zhou, Q.; Wang, C.; Li, Q.; Wang, C.; Fang, Y. Toward Intrinsic Graphene Surfaces: A Systematic Study on Thermal Annealing and Wet-Chemical Treatment of SiO₂-Supported Graphene Devices. *Nano Lett.* **2011**, *11* (2), 767–771.
- Frank, O.; Tsoukleri, G.; Parthenios, J.; Papagelis, K.; Riaz, I.; Jalil, R.; Novoselov, K. S.; Galiotis, C. Compression Behavior of Single-Layer Graphenes. *ACS Nano* **2010**, *4* (6), 3131–3138.
- Gao, L. B.; Ren, W. C.; Liu, B. L.; Saito, R.; Wu, Z. S.; Li, S. S.; Jiang, C. B.; Li, F.; Cheng, H. M. Surface and Interference Coenhanced Raman Scattering of Graphene. *ACS Nano* **2009**, *3* (4), 933–939.
- Ling, X.; Zhang, J. First-Layer Effect in Graphene-Enhanced Raman Scattering. *Small* **2010**, *6* (18), 2020–2025.
- Ling, X.; Xie, L. M.; Fang, Y.; Xu, H.; Zhang, H. L.; Kong, J.; Dresselhaus, M. S.; Zhang, J.; Liu, Z. F. Can Graphene be used as a Substrate for Raman Enhancement? *Nano Lett.* **2010**, *10* (2), 553–561.
- Jung, N.; Crowther, A. C.; Kim, N.; Kim, P.; Brus, L. Raman Enhancement on Graphene: Adsorbed and Intercalated Molecular Species. *ACS Nano* **2010**, *4* (11), 7005–7013.
- Ling, X.; Zhang, J. Interference Phenomenon in Graphene-Enhanced Raman Scattering. *J. Phys. Chem. C* **2011**, *115* (6), 2835–2840.
- Li, G. H.; Luican, A.; Dos Santos, J. M. B. L.; Neto, A. H. C.; Reina, A.; Kong, J.; Andrei, E. Y. Observation of Van Hove singularities in twisted graphene layers. *Nat. Phys.* **2010**, *6* (2), 109–113.
- Profumo, R. E. V.; Polini, M.; Asgari, R.; Fazio, R.; MacDonald, A. H. Electron-electron interactions in decoupled graphene layers. *Phys. Rev. B* **2010**, *82* (8), 085443.
- Haran, G. Single-Molecule Raman Spectroscopy: A Probe of Surface Dynamics and Plasmonic Fields. *Acc. Chem. Res.* **2010**, *43* (8), 1135–1143.
- Kalbac, M.; Green, A. A.; Hersam, M. C.; Kavan, L. Tuning of Sorted Double-walled Carbon Nanotubes by Electrochemical Charging. *ACS Nano* **2010**, *4*, 459–469.
- Piscanec, S.; Lazzeri, M.; Robertson, J.; Ferrari, A. C.; Mauri, F. Optical phonons in carbon nanotubes: Kohn anomalies, Peierls distortions, and dynamic effects. *Phys. Rev. B* **2007**, *75* (3), 035427.
- Lazzeri, M.; Mauri, F. Nonadiabatic Kohn anomaly in a doped graphene monolayer. *Phys. Rev. Lett.* **2006**, *97* (26), 266407.
- Morell, E. S.; Correa, J. D.; Vargas, P.; Pacheco, M.; Barticevic, Z. Flat bands in slightly twisted bilayer graphene: Tight-binding calculations. *Phys. Rev. B* **2010**, *82* (12), 121407.
- Gruneis, A.; Attacalite, C.; Rubio, A.; Vyalikh, D. V.; Molodtsov, S. L.; Fink, J.; Follath, R.; Eberhardt, W.; Buchner, B.; Pichler, T. Electronic structure and electron-phonon coupling of doped graphene layers in KC8. *Phys. Rev. B* **2009**, *79* (20), 205106.